Journal of Materials Chemistry A

Accepted Manuscript

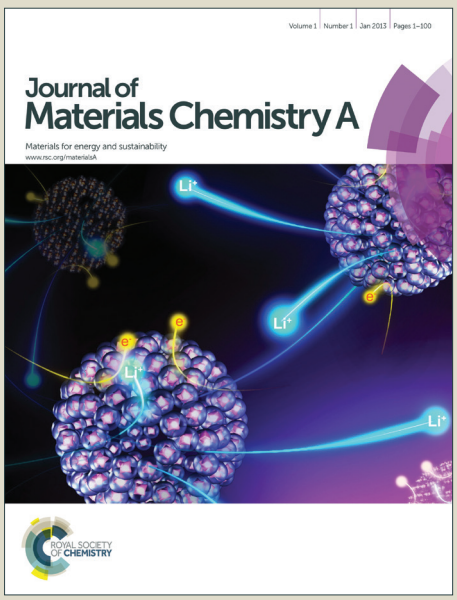

ROYAL SOCIETY OF CHEMISTRY

www.rsc.org/materialsA

Journal of Materials Chemistry A RSCPublishing

ARTICLE

Fabrication of mechanically robust antireflective films using silica nanoparticles with enhanced surface hydroxyl groups

Cite this: DOI: 10.1039/xoxxoooooox

Received ooth January 2012,
Accepted ooth January 2012

DOI: 10.1039/xoxxoooooox

www.rsc.org/

Y. Wang,[a] M. Y. He[a] and R. Y. Chen*[a]

The outdoor application of antireflective (AR) films requires not only high transmittance but also such mechanical properties as good abrasion-resistance, certain AR durability to resist the damage of the harsh environment. In the study, high mechanical performance was achieved by using a binder system in conjunction with the silica nanoparticles (SiO_2-NPs). Hydrogen peroxide (H_2O_2) as a hydroxyl modifier repaired the surface Si-O- bonds of SiO_2-NPs effectively. The density of surface hydroxyl groups of the SiO_2-NPs modified with H_2O_2 (H_2O_2-SiO_2-NPs) was boosted from 1.08 /nm^2 to 2.00 /nm^2, providing an effective route to prepare very robust AR films with abundant Si-O-Si bridging chemical bonds. The addition of linear silicate polymers (SiO_2-LPs) into the silica sols performed the function of a polymer binder and markedly improved the abrasion-resistance and AR durability of the films. The H_2O_2-SiO_2-NP/LP composite films derived from these sols possessed excellent optical and mechanical properties. The average transmittance of the composite films reached 97.5% in the visible spectrum, in contrast to 92.0% for bare glass substrate. Further, the film with a hardness value of 1.7 GPa could pass a 7 H pencil test. Moreover, the relationship between structure and properties of the films was discussed considering the formation mechanism.

1. Introduction

Antireflective (AR) films as the indispensable part of solar photovoltaic[1-3] and solar thermal[4-6] devices can effectively enhance the transmission of sunlight and improve the efficiency of the photoelectric conversion and light-heat conversion. In consideration of the harsh application environment and a service life of at least 20 years for the solar energy devices, the AR films with high transmittance also were required to obtain good abrasion-resistant property to extend the working life and certain AR durability to resist the damage of humid environment.

An ideal homogeneous AR film can achieve effectively 0% reflection at a specific wavelength when its refractive index is equal to $(n_a n_s)^{1/2}$, where n_a and n_s are the refractive indices of air and substrate, respectively. A typical glass has a refractive index between 1.45 and 1.65 in the visible spectral region, which implies that the refractive index of an AR film must be between 1.20 and 1.28. The silica AR films[7-10] prepared by sol-gel technique have been widely used in solar energy application fields for their low refractive index, ease of preparation and low cost. The growth of silica sols with an acid catalyzed sol-gel process invariably leads to linear structure with branches. After coating process, with solvent volatilizing, the condensation of silanol (Si-OH) groups and residual oxethyl groups occurs gradually and thus more Si-O-Si chemical bonds are formed. Therefore, acid-catalyzed films demonstrate much better abrasion-resistant property, but dense structure with high refractive index. By introduction templates[11-14] into the silica sols, such as polyethylene glycol (PEG), cetyl trimethyl ammonium bromide (CTAB) and block copolymers, uniformly distributed pores with different diameters would form by phase separation[15-17] in films after high temperature treatment to remove the templates. With the increase of porosity, the refractive index decreases and thus AR effects improve. However, the removal process of templates is adverse to the chemical bonding between films and substrates, resulting in the serious decline of AR durability. Grosso et al.[18] also published work on further strengthening the durability of silica films by modifying silica sol with organic silane. But the organic groups grafted on the surface of films began obvious degradation after 2000 h during the outdoor performance test[19] which implies that the durability of the films modified with organic groups also cannot meet the requirement in the practical application. Base-catalyzed sols, synthesized by the means of the typical Stöber method[20, 21], usually yield to silica particle sols. The interior porosity and the inter-particle voids of the particles afford the films a refractive index of about 1.22, which is close to the square root of the indices of

[a]School of Petroleum & Chemical, Changzhou University, 1 Gehu Road, Changzhou, Jiangsu 213164, PR China

*E-mail: cxdcry@163.com. Tel.: +86-519-86330580. Fax: +86-519-86330580.

common optical substrates (1.46-1.52) and near 100% transmittance can be obtained. But since the individual particles in the films are kept intact only by point-contact forces and the content of surface hydroxyl is limited, the amount of Si-O-Si chemical bonds derived from hydroxyl condensation in the film structure is not enough to provide good abrasion-resistance.[22] In Shen et al. study[23], after NH_3-heat treatment at 200 ℃, abundant Si-O-Si linkages were formed and hence the abrasion-resistance of the film was improved in a large degree. Jiang et al.[24] have demonstrated that the film strength could be significantly improved by introducing polydimethylsiloxane (PDMS) into the silica sol. The polymer binder can link individual particles together by covalent bonds and enhance the particle-to-particle bonding strength. Based on above research works, it is shown that the strength of the film structure and the mechanical property are greatly improved by enhancing or/and building the chemical connections in films.

During the hydrolysis-condensation process of TEOS, the formation of chemical bonds is due to the condensation reactions of dehydration and dealcoholization. The resulting Si-O-Si chemical bonds possess high bond energy, good stability and thus are not easy to be damaged. That is the reason researchers have tried to mix the resultant sols respectively catalyzed by base and acid with different sol ratios to regulate film refractive index and take overall consideration of transmittance and abrasion-resistance. In Moghal et al. study[25], the combination of mesoporous silica nanoparticles and TEOS binder has increased the hardness of the film to 5H. However, our[26] and Jiang[27] studies have shown that because both the resultant sols had respectively completed the hydrolysis and condensation reactions before mixing, hardly any chemical bonds would generate between particles after mixing and the improvement in abrasion-resistance was still limited.

It is well known that the formation of abundant Si-O-Si chemical bonds requires the presence of vast cross-linkable Si-OH on particles surface and the chains of silicate polymers in the process of condensation. In this research, we employed aqueous colloidal silica (ACS) as the silica source. However, it is important to note that a large amount of surface hydroxyl groups of SiO_2-NPs in ACS sol had been damaged and transformed into surface Si-O- bonds in their production process. Thus, hydrogen peroxide (H_2O_2) as a hydroxyl modifier[28] was introduced to repair the surface Si-O- bonds. The density of surface hydroxyl groups and activity of SiO_2-NPs were dramatically improved. Meanwhile, the addition of linear silicate polymers (SiO_2-LPs) into the silica sols performed the function of a polymer binder. A condensation reaction occurred between hydroxyl groups of SiO_2-LPs and surface hydroxyl groups on SiO_2-NPs. As a result, the SiO_2-NPs were covalently linked by SiO_2-LPs, enhancing the abrasion-resistance of AR films. The innovational point of this work is the utilization of H_2O_2 in a simple route to achieve high activity SiO_2-NPs with low aggregation extent and stable AR films with improved abrasion-resistance. The film formation mechanism was investigated in detail, and the relationship between the microstructure and the properties of AR films was proposed.

2. Experimental Section

2.1 Modification of hydroxyl on the surface of SiO_2-NPs. Ludox®TM-50 ACS suspension (Sigma-Aldrich, St. Louis, MO), was used as the silica source, where the silica particle size, the SiO_2 mass content and the pH were 22 nm, 50%, ca.9, respectively. Ludox®TM-50 and H_2O_2 (30%) were mixed under reflux at 108℃ for 5 h with in a molar ratio 1: 5.3, then concentrated at 80℃ to remove H_2O_2. This modified silica sol was coded as sol-A. The final concentration of SiO_2 in sol-A was 30% by weight.

2.2 Preparation of silica sols. Fig. 1 illustrates the main procedure of the preparation of silica sols. Sol-A (modified ACS sol), absolute ethanol (EtOH, 99.9%), concentrated hydrochloric acid (HCl, 36-38%) and tetraethylorthosilicate (TEOS) were mixed and stirred for 6 h at room temperature. The molar ratio was SiO_2: EtOH: HCl: TEOS =1: 30: 0.06: 0~0.6. The resulting silica sol was aged in sealed glass containers at room temperature for 2~3 d. This sol was coded as sol-B. To make a contrast to the films from sol-B and sol-C were synthesized by mixing Ludox®TM-50(unmodified ACS sol), EtOH, HCl and TEOS at 1: 30: 0.06: 0.3 molar ratio. The acid catalyzed sol-gel silica sol (sol-D) as reference[13] was also prepared. EtOH, deionized water (H_2O), HCl and TEOS were mixed at room temperature with in a molar ratio 37: 2: 0.03: 1. All chemicals were used as received without further purification and purchased from Sinopharm Chemical Reagent Co., Ltd. (Shanghai, China).

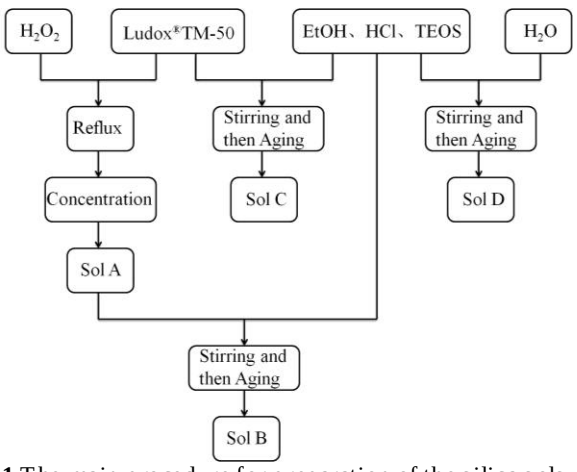

Fig. 1 The main procedure for preparation of the silica sols

2.3 Preparation of silica films. Before the preparation, glass substrates were carefully cleaned in the following procedures: the 3 mm thickness borosilicate glass substrates (100×25 mm^2) were successively treated in base solution and acid solution by ultrasonic for 1 h. The mixed base and acid washing solutions had the volume ratio of H_2O: H_2O_2: $NH_3 \cdot H_2O$ = 5: 1: 1 and H_2O: H_2O_2: HCl = 5: 1: 1, respectively. Then the substrates were completely cleaned up by deionized water and alcohol. Well-cleaned substrates were dry off by blowing with N_2.

Preparation of silica films: The sol-B, sol-C and sol-D were deposited on well-cleaned borosilicate glass substrates by the dip-

coating process at a withdrawal rate of 80 mm/min, respectively. The as-deposited films were pre-dried at 80 ℃ for 30 min and subsequently were heat treated at 400 ℃ for 2 h.

2.4 Characterization. The transmittance spectra in the wavelength range of 400 ~ 800 nm were measured by an UV-visible spectrophotometer (Shimadzu, UV-1700). A UVISEL phase modulated spectroscopic ellipsometer (HORIBA Jobin Yvon) was used to determine the refractive indices of the films. Field Emission Scanning Electron Microscopy (FESEM, SUPRA55, CarlZeiss) and Atomic Force Microscopy (AFM, Veeco, NanoMan VS) were employed to study the detailed morphological surface analysis and roughness of the films. To investigate the structures of the films FTIR absorption spectra were recorded in the 4000 to 400 cm^{-1} range using a Nicolet PROTÉGÉ 460 system, equipped with a DTGS KBr (deuterated triglycine sulphate with potassium bromide windows) detector. The Brunauer-Emmet-Teller (BET, Micromeritics, Tristar II) was used to determine the total specific surface areas. ^{29}Si magic-angle spinning (MAS) NMR spectra[29] were obtained on a UNITY INOVA-500 Spectroscopy using a DOTY Scientific multinuclear probe and 5 mm zirconia rotors and used to investigate the chemical structure of the silica network. ^{29}Si resonance frequency was 99.745 M Hz; pulse width, 4μs; recycle delay time, 400 s; and spinning speed, 8 kHz. Apparent zeta-potential was measured by a Zeta potential analyzer (Malvern, ZEN3600).

The abrasion-resistance of the films was evaluated by a pencil hardness tester.[30, 31] The test conformed to the ISO standard 15184, where a vertical force of 7.5 ± 0.1 N was applied at tip of the pencil. The pencil was fixed at 45˚angle to the horizontal film surface as the pencil was moving over the coated specimen. The pencil lead was flattened before the test as specified in the standard. From soft to hard (6 B to 9 H), the hardest pencil grade that did not cause damage to the coated specimen was termed as the pencil hardness of the film. The existence of the scratches was observed by optical microscope. Furthermore, the hardness of the films was also determined using a nanoindenter (NANO G200, MTS). Before performing any indentation, the indenter was stabilized so that the thermal drift rate was less than 0.05 nm/s. For all indentations, a constant strain rate (0.05 s^{-1}) loading was used. For each sample, a 2 × 2 array with a size of 50 × 50 μm^2 was scanned and statistically analyzed. [32]

2.5 Titration of surface hydroxyl. The density of surface hydroxyl was quantitatively characterized according to Boehm titration[33-35]. Typically, one gram of sample was dispersed in the 100 ml mixture of EtOH and NaCl and then sealed and shaken thoroughly for 24 h. The pH value of the resulting suspension was first adjusted to 4.0 by 0.01 M HCl or 0.018 NaOH and then the pH was further adjusted with the same concentration of NaOH to successive values from 4.0 to 9.0 kept for at least 20s. Finally, according to Eq.1:

$$N=CVN_A\times10^{-3}/Sm$$

in which *C*, *V*, N_A, *S* and *m* are the concentration of NaOH (mol/L), the consumption of NaOH (mL), which cause the pH value of the resulting suspension vary from 4.0 to 9.0, the avogadro constant, the specific surface area of the sample (nm^2/g) and the mass of the sample (g), respectively, the density of surface hydroxyl was calculated out.

3. Results and Discussion

3.1 Modification of SiO_2-NPs surface hydroxyl with H_2O_2. H_2O_2 was used to increase the surface hydroxyl density of the carbon, and make the charge of that surface more negative. The surfaces of the carbon with a higher hydroxyl density and negative charge preserved a higher activity of adsorbed catalase, because less deformation of the enzyme occurred as a result of higher repulsive electrostatic interactions and lower hydrophobic interactions.[28] Thus, H_2O_2 was introduced and expected to increase surface hydroxyl density and activity of SiO_2-NPs in this research. The ACS sol and sol-A were completely dried at 80 ℃ before and after the modification with H_2O_2 and the FTIR absorption spectra of the resulting silica gels are recorded in Fig. 2.

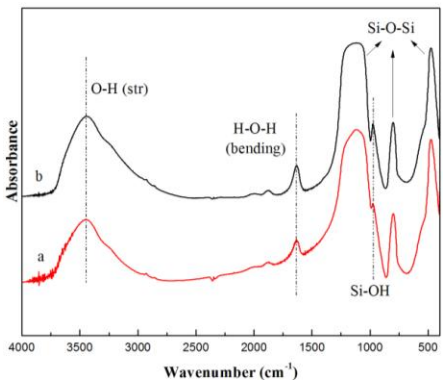

Fig. 2 FTIR spectra of the dried silica gels before and after the modification with H_2O_2: (a) ACS gel; (b) gel-A

The absorption bands observed at around 475, 805 and 1120 cm^{-1} are attributed to antisymmetric stretching vibration, symmetric stretching vibration and bending vibration of the Si-O-Si bonds, [36] respectively. The broad absorption band at around 3438 cm^{-1} is due to the -OH groups and the absorption band at 970 cm^{-1} is associated to the asymmetric stretch vibration of Si-OH.[37] It can be noted here that the peak area of -OH groups in the FTIR spectrum of the gel-A, trace (b) in Fig. 2, is obviously greater than the peak area in the ACS gel trace (a) in Fig. 2. Furthermore, the low-intensity absorption band assigned to Si-OH groups is strongly strengthened in the FTIR spectrum of the gel-A compared to that of the ACS gel. In the FTIR spectrum of the gel-A, the increases in the intensities of -OH absorption peak at around 3438 cm^{-1} and Si-OH absorption peak at around 970 cm^{-1} undoubtedly indicate that the surface hydroxyl density of SiO_2-NPs is significantly improved by the modification of H_2O_2. As expected, the H_2O_2 modification exhibits positive effects on the restoration of surface Si-OH bonds for SiO_2-NPs.

As a strategy to further prove the effects of H_2O_2 modification, the method of Boehm titration and BET analysis were used to provide quantitative information on the density of surface hydroxyl and the specific surface area of the dried silica gels before and after the modification with H_2O_2. The results were calculated according to Eq.1 and presented in Table 1.

As shown in Table 1, the gel-A has a higher surface hydroxyl density of 2.00 /nm^2 compared to the ACS gel (1.08 /nm^2). The growth of the surface hydroxyl density nearly doubles after H_2O_2 modification. The result is in accordance with the FTIR

observation on the difference between Si-OH density. This is highly suggestive that the H_2O_2 modification is a key to repairing the surface Si-O- bonds of SiO_2-NPs and thus the surface hydroxyl density of SiO_2-NPs correspondingly increases. As a result, the higher surface hydroxyl density will greatly boost the amount of cross-linkable particles in silica sol and benefit the reaction activity.

Table 1 The S_{BET} and the density of surface hydroxyl of the dried silica gels before and after the modification with H_2O_2

Gels Samples	S_{BET} (m^2/g)	N_{OH} (nm^{-2})
ACS gel	265.72	1.08
gel-A	302.98	2.00

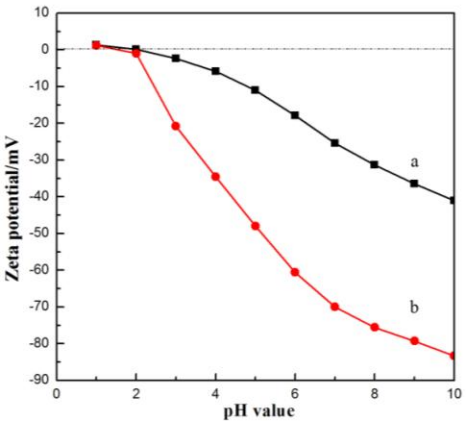

Fig. 3 Effects of pH on zeta potential of SiO_2-NPs before and after the modification with H_2O_2: (a) ACS sol; (b) sol-A

On the other hand, the distribution of charges on the surface of SiO_2-NPs will be no doubt changed because of the replacement of surface Si-O- bonds by Si-OH groups. Fig. 3 gives the zeta potential of both ACS sol and sol-A as a function of pH value. The silica sols all have a negative zeta potential for pH>2, with the absolute value of the zeta potential increasing with increasing pH value. For unmodified ACS sol, the absolute value of the zeta potential is smaller than 45 mV. It demonstrates the low dispersability of particles in ACS sol that is clearly a result of the low surface charges on particles, which is insufficient in preventing particles aggregation and precipitation. On the contrary, the sol-A has a high zeta potential value over a wide pH range (5-10). It suggests that it is the presence of the surface hydroxyl and concomitant surface charges that enable the efficient dispersal of particles in silica sol. Furthermore, the isoelectric point (IEP) is the pH of a dispersion medium of a colloidal suspension at which the colloidal particles carry no net charge. The colloidal system is the least stable at the IEP as there are no inter-particle repulsive forces due to absence of particle surface charges. In case of the ACS sol the IEP is approximately 2 and is about 1.5 for the sol-A. The difference in the IEP is also due to different zeta potential of the particles. The modification of H_2O_2 makes the zeta potential of the particles significantly increase and then enhances repulsive electrostatic interactions between particles.[38] Thus, the particles with high surface charges exhibit good dispersability and stability in silica sol, which can availably prevent from the aggregation and precipitation of particles. Besides, the data in Table 1 show that the specific surface area of silica gel also increases after the modification with H_2O_2 indicating the improvement of aggregative phenomenon.

Due to introduction of H_2O_2 in sol, the H_2O_2-SiO_2-NPs possess high activity and reveal outstanding dispersability and stability, which not only improves the degree of hydroxyl condensation among particles, but promote the formation of homogeneous films.

3.2 Effects of the H_2O_2 modification on the chemical bonding between SiO_2-NPs and SiO_2-LPs. In order to confirm the existence of the strong interaction between SiO_2-NPs and SiO_2-LPs that can enhance the mechanical properties of films, solid-state ^{29}Si MAS NMR was used (Fig. 4). The sol-B, sol-C derived from the H_2O_2-SiO_2-NPs and the SiO_2-NPs respectively and sol-D prepared by the acid catalyzed sol-gel process were pre-dried at 80 ℃ and subsequently were heat treated at 400 ℃ for 2 h. The solid state ^{29}Si MAS NMR spectra of the resulting silica gels are revealed in Fig. 4. The signals around -80, -87, -98 and -110 ppm are assigned to Si in Q^1 ($Si^*(OSi)(OH)_3$), Q^2 ($Si^*(OSi)_2(OH)_2$), Q^3 ($Si^*(OSi)_3OH$) and Q^4 ($Si^*(OSi)_4$), respectively.[39,40] The silicon sites are labeled with the conventional Q^n notation. Q^n represents a silicon atom with four potential reactive groups. The "n" index represents the number of other silicon atoms bonded to the first silicon by an oxygen bridging atom. Bulk siloxane silicon (Q^4) is connected to four other silicon atoms through adjacent oxygens, while silicon atoms possessing a single hydroxyl group (single silanols) are designated Q^3, and those possessing two hydroxyl groups are designated Q^2 (geminal silanols), etc. The change in the chemical environments of the silicon atom results in a displacement of the chemical shift.

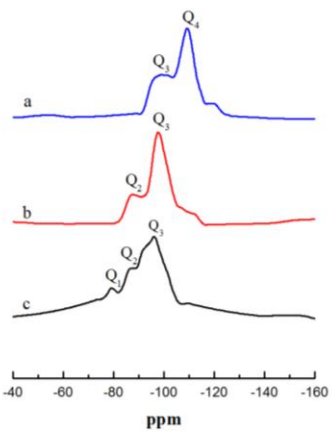

Fig. 4 Change in solid state ^{29}Si MAS NMR spectra for dried and calcined silica gels: (a) gel-B; (b) gel-C; (c) gel-D

It is well known that ^{29}Si chemical shift strongly depends on the polymerization degree of silicon. The total range of ^{29}Si chemical shifts in silicates is appreciable, from -60 to -120 ppm, with analytically significant subdivision into well-separated ranges for monosilicates (Q^0), disilicates and chain end groups (Q^1), middle groups in chanins (Q^2), chain branching sites (Q^3),

and the three-dimensional cross-linked framework (Q^4). Noticeably, all spectra in Fig. 4 exhibit distinct signals, corresponding to different environments of silicon atoms. The major constituents are Q^1, Q^2 and Q^3 for gel-D. It means that condensation of the silicon-oxygen tetrahedral (SiO_4) proceeds and transforms into SiO_2-LPs with low polymerization degree. This result is in agreement with the mechanism of acid catalyzed hydrolysis of TEOS. The acid catalyzed hydrolysis proceeds by a mechanism which involves electrophilic attack on an alkoxide oxygen and, thus, is not particularly sensitive to the electronic effects of the other groups bonded to silicon but would be sensitive to steric effects. Accordingly, monomers are more rapidly hydrolyzed than end groups of chains, which in turn are more rapidly hydrolyzed than the middle groups of chains. The silanols on these weakly cross-linked units then condense more rapidly than silanols on more highly cross-linked species are formed, and the resulting SiO_2-LPs are relatively small and not highly cross-linked. However, it should also be noted that the SiO_2-LPs would have a high activity and great strength and flexibility to bend, rotate as a result of chemical bonding. For the gel-C (Fig. 4b), although the chemical shift is slightly shifted toward negative direction, the silica gel also contains lower cross-linked Q^2 and Q^3 species. Because of the low activity and dispersability, the SiO_2-NPs are very difficult to react with the SiO_2-LPs. Therefore, the SiO_2-LPs with high activity have a tendency both to grow and to condense internally leading to the formation of a network structure of linear chains with polymerization degree.

However, in the solid-state ^{29}Si MAS NMR spectrum (Fig. 4a) of gel-B, significant differences are observed by comparing with the gel-C. There has a marked negative chemical shift. Except for the chain branching sites Q^3, a relatively sharp peak at approximately -110 ppm associated to the three-dimensional cross-linked framework Q^4 firstly emerged in Fig. 4a. As previously discussed, the H_2O_2-SiO_2-NPs with high surface hydroxyl density exhibit excellent reaction activity, which are easy to react with the SiO_2-LPs. And the condensation reaction of both H_2O_2-SiO_2-NPs and SiO_2-LPs not only can form the linear polymer, but further crosslink to get a three-dimensional network structure with higher degree of polymerization.

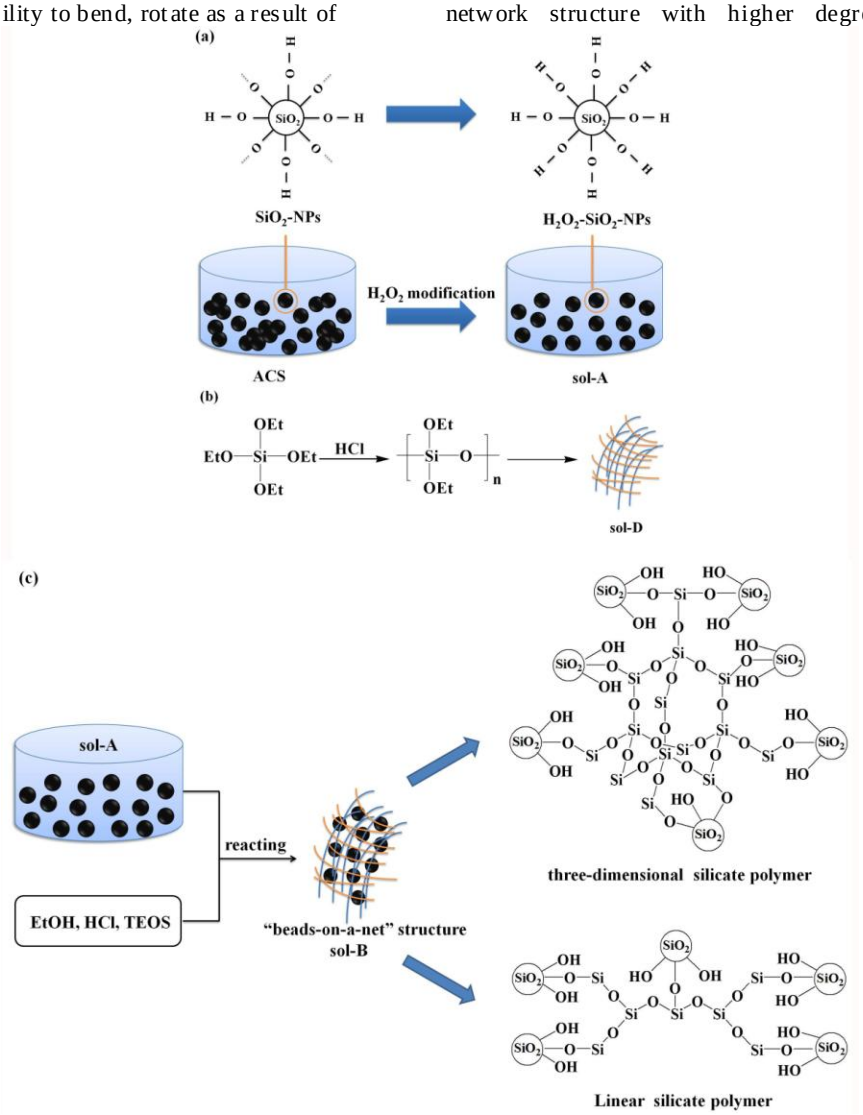

Fig. 5 Schematic diagram of the H_2O_2-SiO_2-NPs/LPs composite film forming process from sol-A modified with H_2O_2 (a), acid-catalyzed sol-D (b), and sol-B (c)

The SiO_2-LPs prepared by an acid catalyzed sol-gel process which contain abundant hydroxyl groups, possess higher activity (Fig. 5b). While the H_2O_2-SiO_2-NPs subjected to the modification of H_2O_2 also are covered with the highly active hydroxyl groups (Fig. 5a). In the H_2O_2-SiO_2-NP/LP composite sol, a little attractive interaction between SiO_2-LPs and H_2O_2-SiO_2-NPs is induced by weak hydrogen bonding of hydroxyl groups of SiO_2-LPs with hydroxyl groups on the H_2O_2-SiO_2-NPs surface. The linkages may avoid the droplet formation, leading to the great improvement of the substrate affinity and film formability during the deposition process. With the subsequent calcination, polycondensation among SiO_2-LPs, H_2O_2-SiO_2-NPs and the glass substrate surface occurs by dehydroxylation reaction leading to branched structure of films. During the condensation process, these high-strength SiO_2-LPs chains are successfully grafted on the surface of H_2O_2-SiO_2-NPs via bulk Si-O-Si bridging chemical bonds. SiO_2-LPs acts as "bridges" between H_2O_2-SiO_2-NPs and links H_2O_2-SiO_2-NPs together, resulting in a "beads-on-a-net" structure as shown in Fig. 5. Furthermore, the resulting films undergo significant densification which is caused by the further aggregation of the "beads-on-a-net" structures, and thus the H_2O_2-SiO_2-NPs/LPs composite film with three-dimensional network structure is prepared as illustrated in Fig. 5c. The highly branched structure of the H_2O_2-SiO_2-NP/LP composite film leads to effective cross-linked between H_2O_2-SiO_2-NPs as well as the glass substrate surface by firm Si-O-Si bridging chemical bonds, making it possible to acquire excellent mechanical property such as abrasion-resistant property.

3.3 Effects of the H_2O_2 modification on surface morphology and abrasion-resistant property of films. The comparisons of the surface morphologies of the H_2O_2-SiO_2-NP/LP composite film and the SiO_2-LP/NP composite film with and without the H_2O_2 modification were analyzed by FESEM and AFM. As can be seen from the Fig. 6A-D, the H_2O_2-SiO_2-NP/LP composite film is composed of the approximate 20 nm spherical silica particles and demonstrates a relatively compact, smooth and uniform surface morphology with sparse pores. Meanwhile, the AFM images of the H_2O_2-SiO_2-NP/LP composite film (Fig. 7A-B) also show that the surface is dense and smooth and its Rq, Ra values are 3.93, 3.19 nm, respectively (Table 2), which can be related to the good uniformity of the film. This surface morphology can be well explained by the SiO_2-LPs bridges model in which the abundant H_2O_2-SiO_2-NPs with high dispersability and activity are linked together by SiO_2-LPs chains. Consequently, the individual H_2O_2-SiO_2-NPs and SiO_2-LPs are chained in series by firm Si-O-Si bridging chemical bonds to form uniform, complete and cross-linked network structure, which consequentially improve the surface morphology of the film. For the H_2O_2-SiO_2-NP/LP composite sol, the twining mode, on one hand, strengthens the binding forces between two forms of silica by strong chemical bonds, instead of weak physical bonds; on the other hand, the "beads-on-a-net'' structure creates after twining and condensation of silanol groups, which prevents the existence of particles clusters or particles from being greatly raised on the surface. What is more, the "beads-on-a-net'' structure can spread out very well on the glass substrate, thus the abrasion-resistant property of the H_2O_2-SiO_2-NP/LP composite film is strengthened. A pencil hardness measurement (ISO 15184) is one of the standard industrial tests in determining the abrasion-resistant property of a surface coating. Therefore, the abrasion-resistant property of films was evaluated by performing pencil hardness measurements. The existence of the scratches also was observed by optical microscope and presented in Fig. 8. For the H_2O_2-SiO_2-NP/LP composite film, there exists slight scratch damage even if the pencil for test is 8 H (Fig. 8B). According to the standard, the pencil hardness grade of the H_2O_2-SiO_2-NP/LP composite film can reach 7 H (Table 2), which is in very good agreement with the above argument. Comparing the 8 H hardness of the sol-gel acid catalyzed film derived from sol-D, we can draw a conclusion that the addition of SiO_2-LPs, which acts as a polymer binder, to the silica sol leads to the formation of the highly crosslinked network structure, and the abrasion-resistant property of the H_2O_2-SiO_2-NP/LP composite film is improved. Fig. 6D shows the FESEM cross-sectional image of the H_2O_2-SiO_2-NP/LP composite film which has a constant thickness of 135 nm. This value is consistent with the maximum transmittance in the wavelength range of about 550-650 nm exhibited in Fig. 9.

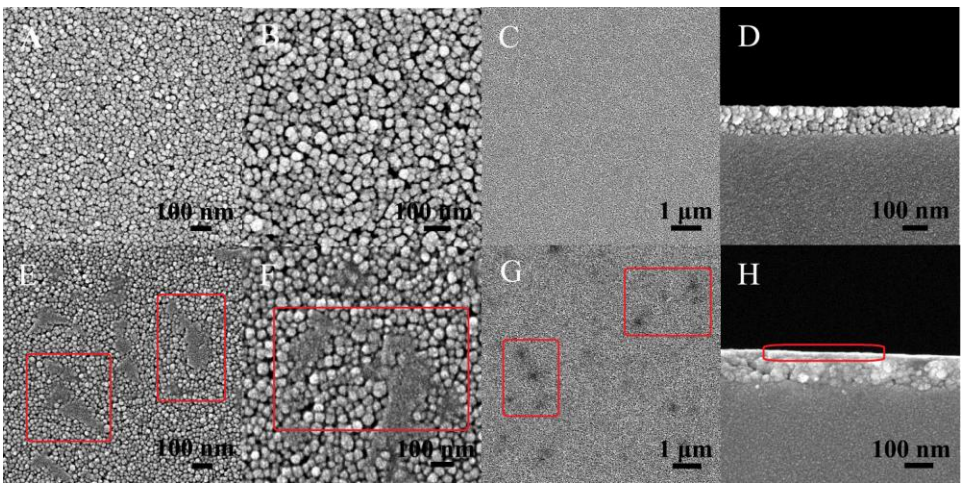

Fig. 6 The FESEM surface and cross-sectional images of the silica films with and without the H_2O_2 modification: (A-D) H_2O_2-SiO_2-NP/LP composite film; (E-H) SiO_2-NP/LP composite film

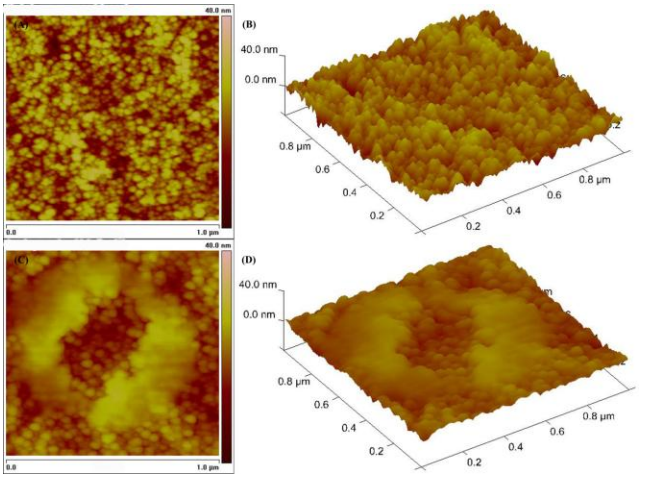

Fig. 7 The AFM images of the silica films with and without the modification of H_2O_2: (A-B) H_2O_2-SiO_2-NP/LP composite film; (C-D) SiO_2-NP/LP composite film

Table 2 Roughness parameters, pencil hardness grades and film thicknesses of the H_2O_2-SiO_2-NP/LP, SiO_2-NP/LP composite films and sol-gel acid catalyzed film

	SiO_2-NP/LP composite film	H_2O_2-SiO_2-NP/LP composite film	sol-gel acid catalyzed film
Rq (nm)	3.01	3.93	0.473
Ra (nm)	2.37	3.19	0.377
Rmax (nm)	28.6	31.5	3.92
Pencil hardness grade	3 H	7 H	8 H
Film thickness (nm)	125	135	120

Where Rq is the root mean square (RMS) roughness, the most widely used amplitude roughness parameter; Ra is the mean deviation of height; Rmax is the height of peak to vally

The FESEM images of the SiO_2-NP/LP composite film are shown in Fig. 6E-H. Besides of the aggregation of massive particles, large-scale dense regions are also observed on the surface of the SiO_2-NP/LP composite film indicating that the uniformity of the film declines. Moreover, this phenomenon still exists in the AFM images of the SiO_2-NP/LP composite film (Fig. 7C-D). According to the date in Table 2, the roughness parameters Rq, Ra of the SiO_2-NP/LP composite film are 3.01 nm and 2.37 nm, respectively, which are obviously less than the surface roughness of the H_2O_2-SiO_2-NP/LP composite film. This result can be interpreted as due to the low chemical crosslinked between SiO_2-NPs and SiO_2-LPs is attributed to low surface hydroxyl density and activity of the SiO_2-NPs unmodified with H_2O_2. Hence, it is difficult for most of SiO_2-NPs to participate in the dehydroxylation reaction. The SiO_2-LPs with high activity condense preferentially with each other rather than the SiO_2-NPs, giving rise to the densification of surface morphology and the decrease of surface roughness. This result is consistent with the conclusion of ^{29}Si MAS NMR. For the SiO_2-NP/LP composite film, there are only point-contact forces between the particles, and the binding forces within the film are therefore quite weak. As can be seen from the Fig. 8A, although with the 4 H pencil grade, the SiO_2-NP/LP composite film has notable scratch damage. Thus, the pencil hardness grade of the SiO_2-NP/LP composite film is only 3 H. Moreover, the FESEM cross-sectional imageof the SiO_2-NP/LP composite film (Fig. 6H) reveals that the thickness of the film is about 125 nm.

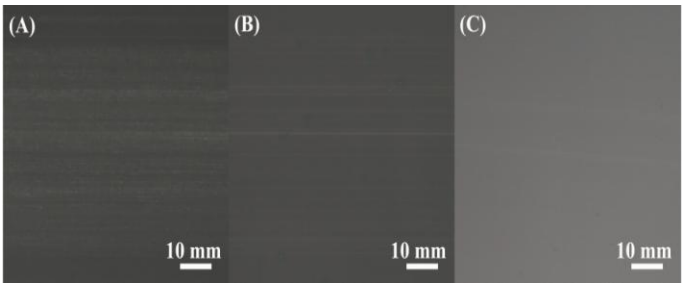

Fig. 8 Hardness of films after the pencil hardness test: (a) 4 H pencil causes damage to the SiO_2-NP/LP composite film, (b) 8 H pencil causes damage to the H_2O_2-SiO_2-NP/LP composite film, (c) 9 H pencil causes damage to the sol-gel acid catalyzed film (original magnification = ×40)

Besides the pencil hardness measurements, the mechanical property was also investigated using nanoindenter measurements to provide quantitative information on hardness, based on the conventional Oliver-Pharr method.[32] Comparing the nanoindentation hardness of the H_2O_2-SiO_2-NP/LP composite film (1.7 GPa) with that of SiO_2-NP/LP composite film (0.9 GPa), it is seen that the former shows dramatically higher hardness than the latter thereby imparting better abrasion-resistant for day-to-day handling.

3.4 Effects of the addition of SiO_2-LPs on optical and abrasion-resistant properties of the H_2O_2-SiO_2-NP/LP composite films. The variations of AR effects for the H_2O_2-SiO_2-NP/LP composite films with different SiO_2: TEOS molar ratios are shown in Fig. 9. The transmittance of all films distribute as a wave mountain in the visible spectrum (400-800 nm), reach its maximum at around 600 nm and decay gradually toward the edge. This transmittance behavior is determined by the nature of the homogeneous single-layer AR film. According to the principle of AR, the ideal homogeneous single-layer AR film can achieve effectively zero reflectance at a specific wavelength when its film thickness is equal to a quarter of the specific wavelength. The H_2O_2-SiO_2-NP/LP composite films belong to the homogeneous single-layer AR film and have the constant film thickness. Thus, the H_2O_2-SiO_2-NP/LP composite films can reduce the reflection effective to a very low level, but only for the specific wavelength. The reflected light derived from other wavelength will be weakened in some degree. As a result, the transmittance maximization only can be realized at a relatively narrow spectral range, as shown in Fig. 9. The film thicknesses of the H_2O_2-SiO_2-NP/LP composite films range from 135 nm to 151 nm. Therefore, the maximum transmittance should be obtained at 540-604 nm, which is in accordance with the results of Fig. 9 (550-650 nm).

Furthermore, as seen, the transmittance of all films in the visible spectrum is visibly enhanced by comparing with that of the bare glass substrate. When the SiO_2: TEOS molar ratio ranges from 1: 0 to 1: 0.6, the transmittance of the H_2O_2-SiO_2-NP/LP composite film shows a gradual downward trend. Furthermore, the data in Table 3 also reveal that with the increase of the addition of SiO_2-LPs, the average transmittance in the visible spectrum decreases in turn from 98.8% to 94.7%, whereas the pencil hardness grade of corresponding film increases. As the SiO_2: TEOS molar ratios are 1: 0.5 and 1: 0.6, the hardnesses are as high as 8 H.

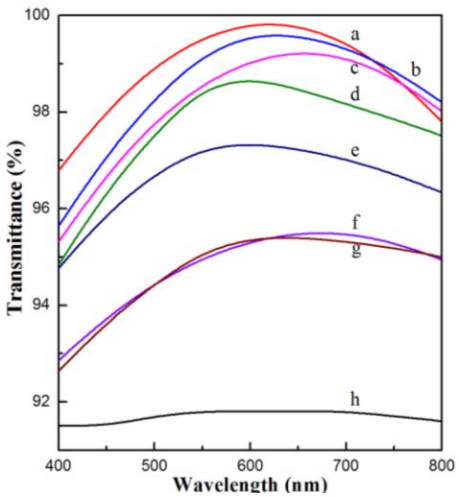

Fig. 9 Effects of the different SiO_2: TEOS molar ratios on optical property of the H_2O_2-SiO_2-NP/LP composite films: (a) 1:0, (b) 1:0.1, (c) 1:0.2, (d) 1:0.3, (e) 1:0.4, (f) 1:0.5, (g) 1:0.6, (h) bare glass substrate

The transmittance of AR films is determined by their refractive indices. According to the Eq.2:

$$n_{pc}^2 = (n_{dc}^2 - 1)(1 - P/100)$$

in which n_{pc} and n_{dc} are the refractive index of the porous and dense silica film respectively and P is the percent porosity, the increase of P would effectively lower the refractive index and enhance the transmittance of films.[41, 42] When the SiO_2: TEOS molar ratio is 1: 0, the H_2O_2-SiO_2-NP/LP composite film composed by abundant H_2O_2-SiO_2-NPs has high porosity and a series of pore structures, which are caused by the particles stack. At 100% particles (no polymer binder SiO_2/LPs) the refractive index of the films is 1.12. The average transmittance in the visible spectrum can reach to 98.8%. However, due to the absence of the polymer binder SiO_2/LPs, only physical forces, instead of chemical bonds, exist between individual particles and with the glass substrate surface and thus the film does not possess excellent abrasion-resistant property. According to the standard, the pencil hardness grade of the film can be defined as less than 6 B. When the addition of SiO_2/LPs increases, more SiO_2/LPs are filled into the pores. The decrease in the porosity is attributed to filling or/and connections or/and bounds between particles in the sol by the linear chains, which results in an increase in refractive index of the films. As shown in Table 3, the refractive index of the H_2O_2-SiO_2-NP/LP composite film increases from 1.17 to 1.42 when the SiO_2: TEOS molar ratio varies from 1:0.1 to 1:0.6. Therefore, the transmittance is reduced accordingly. In contrast, the introduction of SiO_2/LPs leads to highly crosslinked silica framework, making it possible to connect particles with the glass substrate surface via robust Si-O-Si bridging chemical bonds. As the H_2O_2-SiO_2-NPs are linked by the chains of SiO_2/LPs, the abrasion-resistance of the film improves. That is, by increasing the SiO_2/LPs ratio, the sol gives films with lower porosity and solid network structure, and hence reduced AR effects and excellent abrasion-resistance.

Finally, the SiO_2: TEOS molar ratio 1: 0.3 is considered as the optimum preparation conditions for the H_2O_2-SiO_2-NP/LP composite film because the resulting film simultaneously integrates high transmittance with excellent abrasion-resistance. The maximum transmittance is as high as 98.6 % at 590 nm and the average transmittance is 97.5 % in the visible spectrum. The refractive index value of 1.26 also is a better value for zero reflectance. Moreover, the film with 7 H hardness exhibits extremely high abrasion-resistant property. In summary, the addition of SiO_2/LPs serves two functions. First it is used to increase the refractive index of the H_2O_2-SiO_2-NP/LP composite film to the desired value. The second function of the polymer binder SiO_2/LPs is to improve the mechanical properties of the H_2O_2-SiO_2-NP/LP composite film.

Table 3 The average transmittance, pencil hardness grades, refractive indices and film thicknesses of the H_2O_2-SiO_2-NP/LP composite films as a function of different SiO_2: TEOS molar ratios

SiO_2: TEOS molar ratio	1: 0	1: 0.1	1: 0.2	1: 0.3	1: 0.4	1: 0.5	1: 0.6
Average transmittance (%)	98.8	98.4	98.1	97.5	96.6	94.7	94.7
Pencil hardness grade	< 6 B	B	3 H	7 H	7 H	8 H	8 H
Refractive index	1.12	1.17	1.22	1.26	1.33	1.40	1.42
Film thickness (nm)	143	138	151	135	139	145	149

3.5 AR durability of films. AR durability of films is a major determinant in its widespread commercial usage. Fig. 10 shows the average transmittance of the H_2O_2-SiO_2-NP/LP and SiO_2-NP/LP composite AR films as a function of test time in a closed container with 95% relative humidity at room temperature.[43] Obviously, the AR durability is dramatically improved after the modification of H_2O_2. The average transmittance of the SiO_2-NP/LP composite film decreases from 96.3 % to 93.5 %, while that of the H_2O_2-SiO_2-NP/LP composite film remains relatively stable after being tested for 2 months. The AR film subjected to the H_2O_2 modification is more durability, because the highly

crosslinked and very firm silica framework structures are formed by a condensation process between hydroxyl groups of SiO_2-LPs and hydroxyl groups on the H_2O_2-SiO_2-NPs surface and, consequently, the adsorption of water from the environment can be avoided. It also means that the H_2O_2 modification plays a crucial role in preparing the AR film with stable internal structure, outstanding AR durability and abrasion-resistance.

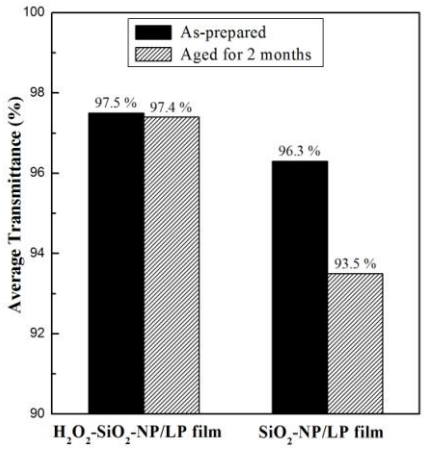

Fig. 10 Change in average transmittance of the silica films as a function of test time

4. Conclusions

The H_2O_2-SiO_2-NP/LP composite sols were prepared by using ACS as the silica source, H_2O_2 as a hydroxyl modifier and SiO_2-LPs derived from the acid catalyzed sol-gel process as a polymer binder. Highly crosslinked H_2O_2-SiO_2-NP/LP composite films with excellent optical property and improved abrasion-resistance and AR durability were obtained. Sol particles with structures of ''beads-on-a-net'' explained successfully the formation mechanism for the H_2O_2-SiO_2-NP/LP composite films. It is found that the modification of H_2O_2 to ACS sols significantly increases the surface hydroxyl density and the activity of the SiO_2-NPs, providing an effective route to prepare highly crosslinked AR films with abundant Si-O-Si bridging chemical bonds. Addition of an appropriate amount of SiO_2-LPs into the silica sols has been shown to markedly improve the abrasion-resistance and AR durability of the films. These AR films with high transmittance, excellent abrasion-resistance and good AR durability simultaneously can be used widely in many optical parts, such as solar collectors.

Acknowledgements

The authors acknowledge the financial support of the Project Funded by the Project supported by National Science Foundation of China (Grant No. 21101017/B0107) and the program granted for the Innovation Project of Postgraduates in Jiangsu Province (CXZZ11-0376).

References

1 B. G. Prevo, E. W. Hon and O. D. Velev, *J. Mater. Chem.*, 2007, **17**, 791-799.
2 L. Zhang, A. Qiao, M. Zheng, Q. Huo and J. Sun, *J. Mater. Chem.*, 2010, **20**, 6125-6130.
3 H. P. Ye, X. X. Zhang, Y. L. Zhang, L. Q. Ye, B. Xiao, H. B. Lv and B. Jiang, *Sol. Energy Mater. Sol. Cells*, 2011, **95**, 2347-2351.
4 A. L. Pénard, T. Gacoin and J. P. Boilot, *Acc. Chem. Res.*, 2007, **40**, 895-902.
5 X. X. Zhang, B. B. Xia, H. P. Ye, Y. L. Zhang, B. Xiao, L. H. Yan, H. B. Lv and B. Jiang, *J. Mater. Chem.*, 2012, **22**, 13132-13140.
6 S. Furbo, S. L. Jivan, *Sol. Energy*, 2003, **74**, 513-523.
7 K. M. A. Sobahan, Y. J. Park, J. J. Kim and C. K. Hwangbo, *Opt. Commun.*, 2010，**18**, 1973-1978.
8 B. G. Kum, Y. C. Park, Y. J. Chang, J. Y. Jeon and H. M. Jang, *Thin Solid Films*, 2011, **519**, 3778-3781.
9 W. Joo, Y. Kim, S. Jang and J. K. Kim, *Thin Solid Films*, 2011, **519**, 3804-3808.
10 M. Manca, A. Cannavale, L. De Marco, A. S. Aricò, R. Cingolani and G. Gigli, *Langmuir*, 2009, **25**, 6357-6362.
11 X. Li, J. Gao, L. Xue and Y. Han, *Adv. Funct. Mater.*, 2010, **20**, 259-265.
12 W. Joo, H. J. Kim and J. K. Kim, *Langmuir*, 2009, **26**, 5110-5114.
13 F. Chi, L. Yan, H. Lv and B. Jiang, *Mater. Lett.*, 2011, **65**, 1095-1097.
14 Q. Liu, J. Zhang, Q. Liu, Z. Zhu and J. Chen, *Mater. Chem. Phys.*, 2009, **114**, 309-312.
15 A. L. Pénard, T. Gacoin and J. P. Boilot, *Acc. Chem. Res.*, 2007, **40**, 895-902.
16 G. Q. Liu, Z. G. Jin, X. X. Liu, T. Wang and Z. F. Liu, *J. Sol-Gel Sci. Technol.*, 2007, **41**, 49-55.
17 S. Walheim, E. Schäffer, J. Mlynek and U. Steiner, *Science*, 1999, **283**, 520-522.
18 M. Faustini, L. Nicole, C. Boissiere, P. Innocenzi, C. Sanchez and D. Grosso, *Chem. Mater.*, 2010, **22**, 4406-4413.
19 J. T. Han, D. H. Lee, C. Y. Ryu and K. Cho, *J. Am. Chem. Soc.*, 2004, **126**, 4796-4797.
20 P. T. Guo, *Adv. Mater. Res.*, 2013, **744**, 269-272.
21 J. D. Brassard, D. K. Sarkar and J. Perron, *ACS Appl. Mater. Interfaces*, 2011, **3**, 3583-3588.
22 X. Wang, J. Shen, *J. Sol-Gel Sci. Technol.*, 2010, **53**, 322-327.
23 X. Li and J. Shen, *Thin Solid Films*, 2011, **519**, 6236-6240.
24 X. Zhang, H. Ye, B. Xiao, L. Yan, H. Lv and B. Jiang, *J. Phys. Chem. C*, 2010, **114**, 19979-19983.
25 J. Moghal, S. Reid, L. Hagerty, M. Gardener and G. Wakefield, *Thin Solid Films*, 2013, **534**, 541-545.
26 X. Meng, Y. Wang, H. Wang, J. Zhong and R. Chen, *Surf. Coat. Technol.*, 2013, **236**, 518-524.
27 H. Ye, X. Zhang, Y. Zhang, L. Ye, B. Xiao, H. Lv and B. Jiang, *Sol. Energy Mater. Sol. Cells.*, 2011, **95**, 2347-2351.
28 R. C. Sosa, R. F. Parton, P. E. Neys, O. Lardinois, P. A. Jacobs and P. G. Rouxhet, *J. Mol. Catal. A: Chem.*, 1996, **110**, 141-151.
29 R. Takahashi, S. Sato, T. Sodesawa, M. Suzuki and K. Ogura, *Bull. Chem. Soc. Jpn.*, 2000, **73**, 765-774.
30 ISO 15184: 1998.
31 Z. Chen, L. Y. L. Wu, E. Chwa, O. *Mater. Sci. Eng. A*, 2008, **493**, 292-298.
32 X. Zhang, P. Lan, Y. Lu, J. Li, H. Xu, J. Zhang, Y. Lee, J. Y. Rhee, K. L. Choy and W. Song, *ACS Appl. Mater. Interfaces*, 2014, **6**, 1415-1423.
33 J. Sears and W. George, *Anal. Chem.*, 1956, **28**, 1981-1983.
34 Z. H. Ou, L. Wu, K. B. Li, S. C. Cao, Y. Wang, L. Lian, D. L. Yi and X.

R. Qin, *Chem. Ind. Eng. Prog.*, 2005, **24**, 1265-1268.
35 H. Wang, M. Tang, K. Zhang, D. Cai, W. Huang, R. Chen and C. Yu, *J. Hazard. Mater.*, 2014, **268**, 115-123.
36 D. Goswami, S. K. Medda and G. De, *ACS Appl. Mater. Interfaces*, 2011, **3**, 3440-3477.
37 S. Cui, Y. Liu, M. Fan, A. T. Cooper, B. Lin, X. Liu, G. Han and X. Shen, *Mater. Lett.*, 2011, **65**, 606-609.
38 P. Leroy, N. Devau, A. Revil and M. Bizi, *J. Colloid Interface Sci.*, 2013, **410**, 81-93.
39 R. Takahashi, S. Sato, T. Sodesawa, M. Kawakita and K. Ogura, *J. Phys. Chem. B*, 2000, **104**, 12184-12191.
40 B. S. Lartiges, J. Y. Bottero, L. S. Derrendinger, B. Humbert, P. Tekely and H. Suty, *Langmuir*, 1997, **13**, 147-152.
41 Y. Xiao, J. Shen, Z. Xie, B. Zhou and G. Wu, *J. Mater. Sci. Technol.*, 2007, **23**, 504-508.
42 G. San Vicente, R. Bayón, N. Germán and A. Morales, *Sol. Energy*, 2011, **85**, 676-680.
43 X. X. Zhang, B. B. Xia, H. P. Ye, Y. L. Zhang, B. Xiao, L. H. Yan, H. B. Lv and B. Jiang, *J. Mater. Chem.*, 2012, 22, 13132-13140.

H_2O_2 modification enables greater interaction between the silica nanoparticles and the linear silicate polymers, thereby increasing mechanical properties and AR durability of the composite films.